FTH1 indicates poor prognosis and promotes metastasis in head and neck squamous cell carcinoma

Qingyun Liao [Equal first author, 1], **Jing Yang** [Equal first author, 2, 3], **Zhaoyi Lu** [4], **Qingshan Jiang** [1], **Yongqian Gong** [1], **Lijun Liu** [1], **Hong Peng** [1], **Qin Wang** [1], **Xin Zhang** [4], **Zhifeng Liu** [Corresp. 1]

[1] Otorhinolaryngology, The First Affiliated Hospital of University of South China, Hengyang, Hunan, China

[2] Cancer Research Institute, Hunan Province Key Laboratory of Tumor Cellular & Molecular Pathology, University of South China, Hengyang, Hunan, China

[3] Gastroenterology, The First Affiliated Hospital of University of South China, Hengyang, Hunan, China

[4] Otolaryngology Major Disease Research, Key Laboratory of Hunan Province, Central South University, Changsha, Hunan, China

Corresponding Author: Zhifeng Liu
Email address: liuzf@usc.edu.cn

Abstract

Background: Currently, ferritin heavy chain (FTH1) has been increasingly found to play a crucial role in cancer as a core regulator of ferroptosis, while its role of non-ferroptosis in head and neck squamous cell carcinoma (HNSCC) is still unclear.

Methods: Herein, we analyzed the expression level of FTH1 in HNSCC using TCGA database, and FTH1 protein in HNSCC tissues and cell lines was determined by immunohistochemistry (IHC) and western blotting, respectively. Then, its prognostic value and relationship with clinical parameters were investigated in HNSCC patients. Additionally, the biological function of FTH1 in HNSCC was explored.

Results: The current study showed that FTH1 is significantly overexpressed in HNSCC tissues and related to poor prognosis and lymph node metastasis of HNSCC. FTH1 knockdown could suppress the metastasis and epithelial-mesenchymal transition (EMT) process of HNSCC.

Conclusion: Our findings indicate that FTH1 plays a critical role in the progression and metastasis of HNSCC and can serve as a promising prognostic factor and therapeutic target in HNSCC.

FTH1 indicates poor prognosis and promotes metastasis in head and neck squamous cell carcinoma

Qingyun Liao[1, *], Jing Yang[2, 3, *], Zhaoyi Lu[4], Qingshan Jiang[1], Yongqian Gong[1], Lijun Liu[1], Hong Peng[1], Qin Wang[1], Xin Zhang[4], Zhifeng Liu[1]

[1]The First Affiliated Hospital, Department of Otorhinolaryngology, Hengyang Medical School, University of South China, Hengyang, Hunan, 421001, China.

[2]The First Affiliated Hospital, Department of Gastroenterology, Hengyang Medical School, University of South China, Hengyang, Hunan, 421001, China.

[3]Cancer Research Institute, Hunan Province Key Laboratory of Tumor Cellular & Molecular Pathology, Hengyang Medical School, University of South China, Hengyang, Hunan, 421001, China.

[4]Otolaryngology Major Disease Research, Key Laboratory of Hunan Province, Xiangya Hospital, Central South University, Changsha, Hunan, 410008, China.

*** These authors contributed equally to this work.**

Corresponding Author:

Zhifeng Liu

Chuanshan Road, Hengyang, Hunan, 421001, China.

liuzf@usc.edu.cn

Abstract

Background: Currently, ferritin heavy chain (FTH1) has been increasingly found to play a crucial role in cancer as a core regulator of ferroptosis, while its role of non-ferroptosis in head and neck squamous cell carcinoma (HNSCC) is still unclear.

Methods: Herein, we analyzed the expression level of FTH1 in HNSCC using TCGA database, and FTH1 protein in HNSCC tissues and cell lines was determined by immunohistochemistry (IHC) and western blotting, respectively. Then, its prognostic value and relationship with clinical parameters were investigated in HNSCC patients. Additionally, the biological function of FTH1 in HNSCC was explored.

Results: The current study showed that FTH1 is significantly overexpressed in HNSCC tissues and related to poor prognosis and lymph node metastasis of HNSCC. FTH1 knockdown could suppress the metastasis and epithelial-mesenchymal transition (EMT) process of HNSCC.

Conclusion: Our findings indicate that FTH1 plays a critical role in the progression and metastasis of HNSCC and can serve as a promising prognostic factor and therapeutic target in HNSCC.

Keywords: HNSCC (head and neck squamous cell carcinoma), FTH1 (ferritin heavy chain), Prognosis, Metastasis, Biomarker

1 Introduction

Head and neck cancers are the sixth most common tumor globally, arising in the upper respiratory tract, of which squamous cell carcinoma accounts for about 90% (Bray et al. 2018). The pathogenesis of the incidence of HNSCC between Occident and China is very different. The leading causes of HNSCC in China are smoking and drinking, while the incidence of HNSCC caused by HPV infection has increased, especially oropharyngeal squamous cell carcinoma in the Occident (Chaturvedi et al. 2011). The incidence of HNSCC is increasing globally, but the continuous development of traditional surgery, radiotherapy, chemotherapy, targeted therapy and even immunotherapy have failed to improve the 5-year survival rate of patients significantly. Compared with HPV-positive patients, the treatment prognosis of negative patients is relatively poor, which prompts scientists to seek personalized treatment based on individual patients' genomic information (Johnson et al. 2020; Network 2015). An in-depth understanding of the molecular biological mechanisms of HNSCC will help discover new molecular biomarkers and potential targets, also provide a basis for early diagnosis and precise treatment.

In 1937, Laufberger isolated a new protein from horse spleen with iron content as high as 23% of dry weight, called ferritin (Laufberger 1937). Although there were some reports of ferritin found in human serum, it was not until 1972 that Addison used immunoradiometric assay to confirm that ferritin does exist in human serum (Addison et al. 1972). Ferritin is composed of 24 middle-hollow round subunits, including heavy chain (FTH1) and light chain (FTL1) (Arenas-Salinas et al. 2014; Goralska et al. 2005). Ferritin plays essential functions such as iron metabolism, signal transduction, immunity, angiogenesis and inflammation, and plays a vital role in many diseases and even tumors (Hazard & Drysdale 1977; Wang et al. 2010). Dysregulated iron metabolism is a tumor Hallmark (Torti & Torti 2013). In HNSCC, it was first reported by Peter in 1986 that ferritin may be a valuable tumor biomarker. In the serum of HNSCC patients, the ferritin content was significantly higher than in the healthy group and the ferritin content in advanced patients was also much higher than that in early-stage patients. There is evidence that the ferritin content in HNSCC patients decreased significantly after receiving successful treatment for five months and returned to normal after five years (Hu et al. 2019). Among the genes encoding the light and heavy chain proteins in ferritin, only FTH1 has ferroxidase activity, while FTL1 is mainly related to iron nucleation and the stability of assembled ferritin (Arosio & Levi 2002). Recent proteomics studies of some tumors have found that ferritin is mainly present in the form of ferritin H in malignant tissues (Lukina et al. 1993). In recent years, FTH1 as a master regulator of ferroptosis has been reported as a prognostic factor in brain cancer, pancreatic cancer, kidney cancer and breast cancer (Chekhun et al. 2014; Huang et al. 2019; Rosager et al. 2017; Su et al. 2017). However, the prognostic value and biological function of FTH1 in HNSCC is still worth further exploration.

Herein, we aimed to clarify the clinical significance and biological function of FTH1 in HNSCC. The results reveal that the expression of FTH1 in cancer was elevated compared to adjacent tissues and FTH1 overexpression indicated a higher risk of lymph node metastasis and poor prognosis of

patients with HNSCC. Furthermore, FTH1 deletion dramatically inhibited the metastasis and EMT of HNSCC cancer cells. Collectively, the current study suggests that FTH1 represented a novel prognostic and metastatic biomarker and a potential therapeutic target for HNSCC. A preprint has previously been published (Liu et al.).

2 Materials & methods

2.1 Data acquisition and tissue specimens

A workflow framework of this research is presented in **Figure 1**. The RNA-Seq and clinical data of HNSCC dataset (528 cases) were downloaded from The Cancer Genome Atlas (TCGA) database. A total of 499 HNSCC samples, with 41 cases of matched adjacent normal tissues, without missing expression and missing follow-up were selected for the subsequent analysis. Besides, 21 sets of HNSCC tissue sections including cancer and adjacent normal tissues used for Immunohistochemistry (IHC) were collected from the First Affiliated Hospital of the University of South China. None of the patients received any preoperative anticancer treatment before surgical procedures. Their pathological diagnosis was confirmed by at least two pathologists. This study was approved by the Medical Ethics Committee of The First Affiliated Hospital of University of South China (Number: 2021ll0916001) and the requirement of consent was waived for the retrospective analysis.

2.2 Immunohistochemistry (IHC)

IHC was performed as our previous studies (Deng et al. 2020; Gong et al. 2018), using the PV-9000 IHC Reagent (ZSGB-BIO, Beijing, China). In brief, tissue sections were dewaxed with turpentine and then hydrated with a gradient of decreasing concentration of ethanol. The antigen retrieval was executed by boiling 10 mmol/l citric acid buffer (pH 6.0) for 15 min. After endogenous peroxidase was inactivated, the sections were blocked with normal goat serum (ZSGB-BIO, Beijing, China) for 10 min. Then the sections were incubated overnight with anti-FTH1 antibody (Affinity, 1:200) at 4 °C, followed by the horseradish peroxidase labeled secondary antibody. For the negative control, the normal rabbit IgG was applied. Finally, the positive signals were visualized by chromogenic agent DAB and nuclei were counter-stained with hematoxylin. Signal strength was scored as follows: 0 (negative), 1(weak), 2 (moderate) and 3 (strong). The staining distribution score is based on the percentage of positive cells: 0 (0-5%), 1 (5-24%), 2 (25-49%), 3 (50-74%) and 4 (75-100%).

2.3 Cell culture and transfection

HNSCC cell lines (Fadu, SCC4, Cal27, HN8 and Cal33), 293T and immortalized non-malignant cell line DOK were obtained from Shanghai Cell Bank (The Chinese Academy of Science, Shanghai) or ATCC. DOK cells were cultured with RPMI 1640 (Gibco). HNSCC cell lines and 293T cells were cultured in DMEM (Gibco). The culture mediums were supplemented with 10% FBS (Gibco) and all cells were cultured at 37 °C with 5% CO_2.

The shRNA-encoding lentiviral vectors for FTH1 knockdown were purchased from GeneCopoeia (GeneCopoeia, Rockville, USA). The shRNA target sequences for human FTH1 were as follows: shFTH1-1: 5′-CCATGTCTTACTACTTTGACC-3′; shFTH1-2: 5′-CCATCAAAGAATTGGGTGACC-3′. The procedures of lentivirus packaging were performed

using Lenti-Pac™ HIV lentivirus packaging kit (GeneCopoeia, Rockville, USA). The negative control, nominated as Lv-control, was packaged with the empty vector. After 48-72 hours of transfection, lentiviral particles were harvested to infect cell lines. Stable transfected cells were selected with puromycin (GeneCopoeia, 2 μg/ml) for 2 weeks and the inhibitory efficiency of FT H1 was confirmed by Western blotting.

2.4 Cell migration and invasion

Cell migration and invasion assay was conducted using wound healing and Transwell invasion assays as reported in our previous studies (Liu et al. 2020; Yang et al. 2020). For wound healing assay, stable transfected cells were seeded in a 6-well plate and scratched using a 10 μl tip when cells reached 90% confluency and then cells were cultured using serum-free medium for 48 h. Transwell invasion assays were performed using Transwell chambers (Corning, USA) pre-coated with 15% Matrigel (Corning, USA). Cells were seeded into the upper chamber (2×10^4 cells/well), while the lower chamber was placed with the medium containing 10% FBS. After 48 hours, the cells on the lower surface were fixed utilizing paraformaldehyde and stained using crystal violet. After removing the cells on the upper surfaces, the stained cells were counted under a microscope.

2.5 Gene Set Enrichment Analysis (GSEA)

Gene set enrichment analysis (GSEA) was performed using GSEA 4.0.1 software to explore the potential functions enriched in subgroups of high or low expression of FTH1. The gene set 'c2.cp.kegg.v7.4. symbols.gmt [curated]' from the MSigDB database was used as reference for GSEA. The enriched sets with P-value < 0.05 and FDR (false discovery rate) < 0.25 were considered statistically significant.

2.6 Western blotting

Whole-cell proteins were extracted using RIPA lysis buffer (NCM Biotech, China) with the proteasome inhibitor (Beyotime Biotechnology, China) and centrifugated to collect the supernatant. After determination of the protein concentration, the collected supernatant was added with SDS buffer, incubated for 10 min at 100 °C, separated by SDS-PAGE and then transferred to the PVDF membrane (Millipore, Bedford, MA). The membranes blocked with 5% skimmed milk was incubated overnight with primary antibody against FTH1 (1:1000 dilution, Affinity), E-cadherin (1:2000 dilution, Proteintech), N-cadherin (1:1000 dilution, CST), Vimentin (1:1000 dilution, CST) at 4 °C. Finally, the antigen-antibody complexes were visualized using enhanced chemiluminescence reagents (Thermo Fisher Scientific).

2.7 Statistical analysis

All statistical analyses were performed using R software (v4.1.0). Student's t test and Wilcox test were used to evaluate differences between two groups. Kruskal Wallis test and one-way analysis were used to analyze differences among multiple groups. Overall survival (OS) and disease-free survival (DFS) analysis were conducted using the Kaplan-Meier method with the log-rank test. The chi-square test and Fisher's exact test were utilized to analyze the correlation between FTH1 expression and the clinicopathologic parameters. Univariate and multivariate Cox regression analyses were performed to identify independent prognostic factors. A value of $P < 0.05$ indicates statistical significance. *, ** and *** represented $P < 0.05$, $P < 0.01$ and $P < 0.001$, respectively.

3 Results

3.1 Differentially expression and prognostic value of FTH1 and FTL1 in HNSCC

The differential analysis of TCGA-HNSC transcriptome data showed that the expression levels of FTH1 and FTL1 in HNSCC samples were significantly higher than those in adjacent normal samples (**Figure 2A, Supplemental Figure 1A**), which were also confirmed using paired sample analysis (**Figure 2B, Supplemental Figure 1B**). FTH1 in HNSCC cells was overexpressed compared with DOK, an immortalized non-malignant cell (**Figure 2C**). The IHC staining showed that FTH1 protein was highly expressed in HNSCC tissues compared with matched adjacent epithelial tissues (**Figure 2D-F**). Based on FTH1 and FTL1, the coding genes for the heavy chain and light chain of ferritin significantly highly expressed in tumor samples from HNSCC patients, and we further analyzed their clinical prognostic value. In the Kaplan-Meier survival estimate, we found that only high expression of FTH1 in tumors indicates worse OS probability (P = 1.39e-03) and DFS probability (P = 4.054e-05), while FTL1 has no prognostic value (**Figure 3A and B, Supplemental Figure 1C and D**). From the above results, it can be indicated that the expression of FTH1 has the prognostic value of OS and DFS simultaneously and the clinical outcomes of patients with high FTH1 expression are worse.

3.2 Correlation between FTH1 and clinical parameters

We generalized these patients' baseline parameters with age, gender, smoking, drinking history, pathological grade, clinical stage, T/N /M stage, OS and DFS according to the high and low expression levels of FTH1 (**Table 1**). The preliminary correlation between FTH1 expression and clinicopathological features was obtained by logical regression analysis, as shown in **Table 2**. It shows that FTH1 expression is associated with smoking (no vs. yes, P = 0.008), pathological grade (G3&4 vs. G1&2, P < 0.01), N stage (N+ vs. N0, P < 0.01) and clinical stage (Stage III&IV vs. Stage I&II, P < 0.05). After that, we further performed a Wilcoxon signed-rank test on clinicopathological features that distribute in high and low FTH1 expression groups. In addition to the differences in FTH1 expression among patients with a history of drinking (P < 0.001), the results of smoking (no vs. yes, P < 0.05), pathological grading (G3&4 vs. G1&2, P < 0.01), N staging (N+ vs. N0, P < 0.01) and clinical stage (Stage III&IV vs. Stage I&II, P < 0.05) conform to logistic regression (**Figure 4A-I**).

We further performed a stratified Kaplan-Meier analysis for OS and DFS in TCGA-HNSC patients with the differential clinical features related to FTH1 expression. The related results showed that FTH1 expression had the prognostic value of OS (P = 0.004) and DFS (P <0.001) in the G1&2 stage, but not in the G3&4 group (**Figure 5A and B, Figure 6A and B**). FTH1 Expression has prognostic value of OS (both P < 0.05) and DFS (both P < 0.05) whether lymphatic metastasis or not (**Figure 5C and D, Figure 6C and D**); FTH1 Expression has a predictive value of DFS (P = 0.002) but no predictive value of OS (P = 0.072) in the early stage (Stage I&II) population, while in advanced patients, have prognostic value regardless of OS (P = 0.013) or DFS (P = 0.004) (**Figure 5E and F, Figure 6E and F**). Finally, we were pleasantly surprised to find that FTH1 Expression has a good prognostic value for both OS and DFS in smokers (P <0.001), while not in non-smokers (**Figure 5G and H, Figure 6G and H**). From the results of the stratified analysis, we guess that FTH1 Expression has better prognostic value for smokers, advanced and pathologically well-differentiated patients, and its prognostic value is not affected by the status of lymph node metastasis.

3.3 Independent predictive power of FTH1

The Cox regression analysis results of FTH1 expression level and clinicopathological features for OS prognosis have been shown in **Table 3**. Univariate cox analysis showed that metastasis (P = 0.026, HR: 3.721, 95%CI: 1.177-11.764) and FTH1 expression ($P < 0.001$, HR: 1.646, 95%CI: 1.254-2.161) were statistically significant. Moreover, multivariate cox analysis showed that both of them still had good statistical significance (metastasis, $P = 0.031$, HR: 3.547, 95%CI: 1.122-11.214) and (FTH1 expression level, $P < 0.001$, HR: 1.658, 95%CI: 1.252-2.194). The above analysis results indicate that in addition to the independent prognostic value of metastasis, FTH1 expression level can also be used as an excellent independent prognostic factor.

3.4 GSEA reveal FTH1-related pathways and molecular functions

Through GSEA, we explored the differences in the downstream activated signaling pathways between the low and high FTH1 expression groups to search for its potential carcinogenic mechanism. After screening of high expression in the group in MSigDB gene set (c2. Cp. Kegg. V7.1. Symbols. gmt), we found that 24 significant enrichment pathways (FDR < 0.25, NOM p-value < 0.05) are mainly concentrated in six aspects between the degree of enrichment of pathways: energy metabolism, glycometabolism, protein and amino metabolism, other metabolisms, cell adhesion and motility and tumor-associated signal pathways (**Figure 7A-D**).

3.5 FTH1 knockdown suppresses HNSCC metastasis by attenuating EMT

As previously mentioned, FTH1 was associated with lymph node metastasis. Hence, wound-healing and Transwell assays were performed to identify FTH1 affecting migration and invasion capabilities of HNSCC cells. Attractively, FTH1 knockdown suppressed wound healing rates in Fadu and HN8 cells (**Figure 8A-D**). Similar results were obtained in the Transwell invasion assays (**Figure 8E and F**). Furthermore, we investigated molecular markers of EMT by Western blotting. After FTH1 depletion, mesenchymal markers (N-cadherin and vimentin) are suppressed, while the epithelial marker E-cadherin was upregulated (**Figure 9A and B**).

4 Discussion

Currently, FTH1 has attracted much attention as a core regulator of ferroptosis (Tang et al. 2021), but its role of non-ferroptosis in HNSCC is still ambiguous. The current study suggests that the role of FTH1 in tumors depends on the context in which it is present. FTH1 can be used as a tumor promoter in metastatic melanoma cells (Di Sanzo et al. 2011a), brain cancer (Rosager et al. 2017), pancreatic cancer (Su et al. 2017) and a tumor suppressor in non-small cell lung cancer (Biamonte et al. 2018a) and ovarian cancer (Lobello et al. 2016), while the role of FTH1 in breast cancer is still controversial (Aversa et al. 2017b; Chekhun et al. 2014). In this study, we discovered that FTH1 is significantly overexpressed in HNSCC tissues in the TCGA-HNSC database, and further, IHC was used to verify the above results. Simultaneously, we found that the high expression of FTH1 correlated with lymph node metastasis and higher pathological grade and clinical stage can act as an independent predictor of the poor prognosis of HNSCC. The results are consistent with previous studies of FTH1 in multiple solid tumors, except for clinical stage (Ali et al. 2021; Hu et al. 2021a; Hu et al. 2021b; Huang et al. 2019). Hence, we aimed to the biological function of FTH1 in HNSCC, and the results demonstrated that endorsed the metastasis of HNSCC cells. Briefly, the

current study indicates that FTH1 plays a vital role in the pro-oncogenic functions and is a potential biomarker and therapeutic target in HNSCC.

Iron metabolism plays a crucial role in cancer metastasis by affecting some enzymes activities. Iron overload increases the activity of metalloprotease-2/9 (MMP-2/9) activating AP-1 via ERK/Akt pathway (Kaomongkolgit et al. 2008). Increased iron concentration caused by FPN overexpression attenuates the ROS generation and impedes EMT (Shan et al. 2018). The role of ferritin as an important iron metabolism regulator has been extensively studied in tumors. However, there are few studies focusing on ferritin subunits FTH1 and FTL1. Among them, only FTH1 has the enzyme activity to oxidize divalent iron to trivalent iron (Timoshnikov et al. 2015). FTH1 helps the synthesis of ferritin by enhancing the storage of iron in cells and mainly affects tumors' progress by regulating iron metabolism. The ratio of FTH1 and FTL1 in ferritin is specific, and ratio H/L and ferritin are essential for cell survival. These two subunits are not interchangeable, and FTL1 cannot compensate for the function of FTH1 (Ferreira et al. 2001). FTH1 plays an essential role in the regulation of proliferation, angiogenesis, migration, EMT, stemness, inflammation and immunoregulation. At present, the research of FTH1 in tumor pathogenesis mainly exerts its functions by affecting iron metabolism. In the study of the proteomics in human metastatic melanoma cells knocking down FTH1, 200 differential proteins were found, mainly distributed in metabolic pathways related to tumor progression and metastasis (Di Sanzo et al. 2011b). And knockdown FTH1 can inhibit the growth and invasion of melanoma. The regulation of iron depletion by FTH1 can slow down the self-renewal of breast cancer stem cells (Kanojia et al. 2012), while silencing FTH1 in SKOV3 cells can promote the stemness of cervical cancer cells and the up-regulation of NANOG, SOX2, OCT4 (Lobello et al. 2016). After down-regulating FTH1 in breast cancer, cervical cancer and non-small cell lung cancer, cancer cells tend to be in a mesenchyme state, which helps tumor metastasis (Aversa et al. 2017a; Lobello et al. 2016). Here, we found that FTH1 silencing hampers the EMT process in HNSCC cells. Our results illuminate that FTH1 functions as a crucial regulator of EMT to enhance the metastasis of HNSCC.

In addition to regulating iron metabolism, FTH1 also directly acts on oncogenes, oncomiRs and the chemokine pathway. Paola et al. found that iron depletion can up-regulate p53 and induce apoptosis (Dongiovanni et al. 2010). Further studies in NSCLC found that FTH1 regulates miR-125b/p53 axis up-regulates the pro-apoptotic protein BAX down-regulates anti-apoptotic protein Bcl2 by destroying the mitochondrial membrane potential (MMP) and mediating a cascade of enzymatic apoptosis (Biamonte et al. 2018b). Silenced-FTH1 MCF-7 and H460 cells produced a large amount of ROS and activated the CXCR4/CXCL12 signaling pathway, thereby promoting cancer high migration (Aversa et al. 2017a). Our GSEA analysis results suggest that FTH1 may plays an important role in multiple cell adhesion signal pathways, such us ECM receptor interaction, focal adhesion, gap junction and regulation of actin cytoskeleton.

FTH1 is present not only as a biological marker but can also be used in magnetic resonance imaging (MRI) and nanomaterials. In breast cancer, serum biomarkers (CA 15-3) combined with tumor-associated antigens and autoantibodies (heterogeneous nuclear ribonucleoproteins F and FTH1) can improve the accuracy of breast cancer diagnosis (Dong et al. 2013). FTH1 was used as an MRI reporter gene in liver cancer, which can be used for the diagnosis and treatment of early liver cancer; also, with additional iron added, it was more efficient and safer in nasopharyngeal carcinoma (Feng et al. 2012; Genove et al. 2005; Zhou et al. 2020). FTH1 nanoparticles coated with EGF have been successfully applied to breast cancer in vitro and in vivo (Li et al. 2012). The nano-ferritin-HFt-MP-PAS40-Dox packaged with doxorubicin was safely applied to HNSCC,

which had a higher maximum tolerated dose (MTD) and better efficiency (Damiani et al. 2017). Currently, siRNA, miRNA, piRNAs and other carriers can be effective tools for targeted FTH1 in the tumor (Balaratnam et al. 2018), of which H-ferritin siRNA has achieved initial success in improving the curative effect of gliomas in patients receiving chemotherapy (Liu et al. 2011). Although ferritin is present in serum but not synthesized in serum, it is mainly leaked by damaged tumor cells, and tumor cell damage mainly occurs in the advanced stage (Kell & Pretorius 2014), so this may cause the ferritin in serum to be unable to predict early HNSCC. The overexpression of FTH1 in tumor tissues may be a good indicator of its cancer-promoting function. In addition to ferroptosis, upregulation of FTH1 may promote the invasion and metastasis of HNSCC. Therefore, the prognostic value of FTH1 for patients in the advanced stages and even posttreatment is worthy of further attention.

However, some limitations of our research should be acknowledged. Firstly, a larger cohort of patients are required for exploring clinical significance. Additionally, the heterogeneity and subsites of HNSCC deserves further exploration. Furthermore, *in vivo* experiments and validation of intermolecular regulation need to be further completed. Thus, future studies with a larger cohort, *in vivo* experiments in mice and molecular mechanism are warranted to further validate the current results.

5 Conclusions

This study found that the high expression of FTH1, not FTL1, could be an independent predictor of the prognosis of HNSCC. In addition, FTH1 downregulation could weaken the metastasis and EMT process of HNSCC. Henceforth, FTH1 could represent a promising biomarker and have value as a therapeutic target for the inhibition of metastasis in HNSCC.

Data availability

The initial data of HNSCC could be downloaded from TCGA (https://portal.gdc.cancer.gov/).

Conflict of interest

The authors declare that the research was conducted in the absence of any commercial or financial relationships that could be construed as a potential conflict of interest.

Ethical statement

This study does not contain animal experimentation, and has been approved by the Medical Ethics Committee of The First Affiliated Hospital of University of South China (Number: 2021ll0916001), and the requirement of consent was waived for the retrospective analysis.

Funding

This study was supported by grants from the Hunan provincial Health and Family Planning Commission (B202307019501, D202307017081, 202103030223, 20201947, B20180186), the

Hunan Provincial Natural Science Foundation of China (2023JJ30544, 2021JJ40502, 2019JJ50547).

Acknowledgments

A preprint has previously been published (Liu et al.).

Authors' contributions

Zhifeng Liu performed study design and wrote the manuscript; Qingyun Liao and Jing Yang conducted experiment performing and data analysis; Zhaoyi Lu, Qingshan Jiang, Yongqian Gong, Lijun Liu, Hong Peng, Qin Wang and Xin Zhang conducted data interpretations, technical support and depicted the figures. All authors approved the manuscript.

References

Addison G, Beamish M, Hales C, Hodgkins M, Jacobs A, and Llewellin P. 1972. An immunoradiometric assay for ferritin in the serum of normal subjects and patients with iron deficiency and iron overload. *Journal of Clinical Pathology* 25:326-329.

Ali A, Shafarin J, Abu Jabal R, Aljabi N, Hamad M, Sualeh Muhammad J, Unnikannan H, and Hamad M. 2021. Ferritin heavy chain (FTH1) exerts significant antigrowth effects in breast cancer cells by inhibiting the expression of c-MYC. *FEBS Open Bio* 11:3101-3114. 10.1002/2211-5463.13303

Arenas-Salinas M, Townsend PD, Brito C, Marquez V, Marabolli V, Gonzalez-Nilo F, Matias C, Watt RK, López-Castro JD, Domínguez-Vera J, Pohl E, and Yévenes A. 2014. The crystal structure of ferritin from Chlorobium tepidum reveals a new conformation of the 4-fold channel for this protein family. *Biochimie* 106:39-47. 10.1016/j.biochi.2014.07.019

Arosio P, and Levi S. 2002. Ferritin, iron homeostasis, and oxidative damage. *Free radical biology & medicine* 33:457-463.

Aversa I, Zolea F, Ieranò C, Bulotta S, Trotta AM, Faniello MC, De Marco C, Malanga D, Biamonte F, Viglietto G, Cuda G, Scala S, and Costanzo F. 2017a. Epithelial-to-mesenchymal transition in FHC-silenced cells: the role of CXCR4/CXCL12 axis. *Journal of experimental & clinical cancer research : CR* 36:104. 10.1186/s13046-017-0571-8

Aversa I, Zolea F, Ieranò C, Bulotta S, Trotta AM, Faniello MC, De Marco C, Malanga D, Biamonte F, Viglietto G, Cuda G, Scala S, and Costanzo F. 2017b. Epithelial-to-mesenchymal transition in FHC-silenced cells: the role of CXCR4/CXCL12 axis. *Journal of experimental & clinical cancer research : CR* 36:104. 10.1186/s13046-017-0571-8

Balaratnam S, West N, and Basu S. 2018. A piRNA utilizes HILI and HIWI2 mediated pathway to down-regulate ferritin heavy chain 1 mRNA in human somatic cells. *Nucleic Acids Res* 46:10635-10648. 10.1093/nar/gky728

Biamonte F, Battaglia AM, Zolea F, Oliveira DM, Aversa I, Santamaria G, Giovannone ED, Rocco G, Viglietto G, and Costanzo F. 2018a. Ferritin heavy subunit enhances apoptosis of non-small cell lung cancer cells through modulation of miR-125b/p53 axis. *Cell death & disease* 9:1174. 10.1038/s41419-018-1216-3

Biamonte F, Battaglia AM, Zolea F, Oliveira DM, Aversa I, Santamaria G, Giovannone ED, Rocco G, Viglietto G, and Costanzo F. 2018b. Ferritin heavy subunit enhances apoptosis of non-small cell lung cancer cells through modulation of miR-125b/p53 axis. *Cell death & disease*

9:1174. 10.1038/s41419-018-1216-3
Bray F, Ferlay J, Soerjomataram I, Siegel RL, Torre LA, and Jemal A. 2018. Global cancer statistics 2018: GLOBOCAN estimates of incidence and mortality worldwide for 36 cancers in 185 countries. *CA: a cancer journal for clinicians* 68:394-424. 10.3322/caac.21492
Chaturvedi AK, Engels EA, Pfeiffer RM, Hernandez BY, Xiao W, Kim E, Jiang B, Goodman MT, Sibug-Saber M, Cozen W, Liu L, Lynch CF, Wentzensen N, Jordan RC, Altekruse S, Anderson WF, Rosenberg PS, and Gillison ML. 2011. Human papillomavirus and rising oropharyngeal cancer incidence in the United States. *Journal of clinical oncology : official journal of the American Society of Clinical Oncology* 29:4294-4301. 10.1200/JCO.2011.36.4596
Chekhun SV, Lukyanova NY, Shvets YV, Burlaka AP, and Buchinska LG. 2014. Significance of ferritin expression in formation of malignant phenotype of human breast cancer cells. *Experimental oncology* 36:179-183.
Damiani V, Falvo E, Fracasso G, Federici L, Pitea M, De Laurenzi V, Sala G, and Ceci P. 2017. Therapeutic Efficacy of the Novel Stimuli-Sensitive Nano-Ferritins Containing Doxorubicin in a Head and Neck Cancer Model. *Int J Mol Sci* 18. 10.3390/ijms18071555
Deng X, Jiang Q, Liu Z, and Chen W. 2020. Clinical Significance of an m6A Reader Gene, IGF2BP2, in Head and Neck Squamous Cell Carcinoma. *Front Mol Biosci* 7:68. 10.3389/fmolb.2020.00068
Di Sanzo M, Gaspari M, Misaggi R, Romeo F, Falbo L, De Marco C, Agosti V, Quaresima B, Barni T, Viglietto G, Larsen MR, Cuda G, Costanzo F, and Faniello MC. 2011a. H ferritin gene silencing in a human metastatic melanoma cell line: a proteomic analysis. *Journal of proteome research* 10:5444-5453. 10.1021/pr200705z
Di Sanzo M, Gaspari M, Misaggi R, Romeo F, Falbo L, De Marco C, Agosti V, Quaresima B, Barni T, Viglietto G, Larsen MR, Cuda G, Costanzo F, and Faniello MC. 2011b. H ferritin gene silencing in a human metastatic melanoma cell line: a proteomic analysis. *Journal of proteome research* 10:5444-5453. 10.1021/pr200705z
Dong X, Yang M, Sun H, Lü J, Zheng Z, Li Z, and Zhong L. 2013. Combined measurement of CA 15-3 with novel autoantibodies improves diagnostic accuracy for breast cancer. *Onco Targets Ther* 6:273-279. 10.2147/ott.S43122
Dongiovanni P, Fracanzani AL, Cairo G, Megazzini CP, Gatti S, Rametta R, Fargion S, and Valenti L. 2010. Iron-dependent regulation of MDM2 influences p53 activity and hepatic carcinogenesis. *Am J Pathol* 176:1006-1017. 10.2353/ajpath.2010.090249
Feng Y, Liu Q, Zhu J, Xie F, and Li L. 2012. Efficiency of ferritin as an MRI reporter gene in NPC cells is enhanced by iron supplementation. *J Biomed Biotechnol* 2012:434878. 10.1155/2012/434878
Ferreira C, Santambrogio P, Martin ME, Andrieu V, Feldmann G, Hénin D, and Beaumont C. 2001. H ferritin knockout mice: a model of hyperferritinemia in the absence of iron overload. *Blood* 98:525-532. 10.1182/blood.v98.3.525
Genove G, DeMarco U, Xu H, Goins WF, and Ahrens ET. 2005. A new transgene reporter for in vivo magnetic resonance imaging. *Nat Med* 11:450-454. 10.1038/nm1208
Gong Y, Luo X, Yang J, Jiang Q, and Liu Z. 2018. RIPK4 promoted the tumorigenicity of nasopharyngeal carcinoma cells. *Biomed Pharmacother* 108:1-6. 10.1016/j.biopha.2018.08.147
Goralska M, Nagar S, Fleisher LN, and McGahan MC. 2005. Differential degradation of ferritin

H- and L-chains: accumulation of L-chain-rich ferritin in lens epithelial cells. *Investigative ophthalmology & visual science* 46:3521-3529.

Hazard JT, and Drysdale JW. 1977. Ferritinaemia in cancer. *Nature* 265:755-756.

Hu Z-W, Chen L, Ma R-Q, Wei F-Q, Wen Y-H, Zeng X-L, Sun W, and Wen W-P. 2021a. Comprehensive analysis of ferritin subunits expression and positive correlations with tumor-associated macrophages and T regulatory cells infiltration in most solid tumors. *Aging* 13:11491-11506. 10.18632/aging.202841

Hu Z-W, Wen Y-H, Ma R-Q, Chen L, Zeng X-L, Wen W-P, and Sun W. 2021b. Ferroptosis Driver SOCS1 and Suppressor FTH1 Independently Correlate With M1 and M2 Macrophage Infiltration in Head and Neck Squamous Cell Carcinoma. *Frontiers In Cell and Developmental Biology* 9:727762. 10.3389/fcell.2021.727762

Hu Z, Wang L, Han Y, Li F, Zheng A, Xu Y, Wang F, Xiao B, Chen C, and Tao Z. 2019. Ferritin: A potential serum marker for lymph node metastasis in head and neck squamous cell carcinoma. *Oncology letters* 17:314-322. 10.3892/ol.2018.9642

Huang H, Qiu Y, Huang G, Zhou X, Zhou X, and Luo W. 2019. Value of Ferritin Heavy Chain (FTH1) Expression in Diagnosis and Prognosis of Renal Cell Carcinoma. *Medical science monitor : international medical journal of experimental and clinical research* 25:3700-3715. 10.12659/MSM.914162

Johnson DE, Burtness B, Leemans CR, Lui VWY, Bauman JE, and Grandis JR. 2020. Head and neck squamous cell carcinoma. *Nature reviews Disease primers* 6:92. 10.1038/s41572-020-00224-3

Kanojia D, Zhou W, Zhang J, Jie C, Lo PK, Wang Q, and Chen H. 2012. Proteomic profiling of cancer stem cells derived from primary tumors of HER2/Neu transgenic mice. *Proteomics* 12:3407-3415. 10.1002/pmic.201200103

Kaomongkolgit R, Cheepsunthorn P, Pavasant P, and Sanchavanakit N. 2008. Iron increases MMP-9 expression through activation of AP-1 via ERK/Akt pathway in human head and neck squamous carcinoma cells. *Oral Oncology* 44:587-594.

Kell DB, and Pretorius E. 2014. Serum ferritin is an important inflammatory disease marker, as it is mainly a leakage product from damaged cells. *Metallomics* 6:748-773. 10.1039/c3mt00347g

Laufberger V. 1937. Sur la cristallisation de la ferritine. *Soc Chim Biol* 19:1575-1582.

Li X, Qiu L, Zhu P, Tao X, Imanaka T, Zhao J, Huang Y, Tu Y, and Cao X. 2012. Epidermal growth factor-ferritin H-chain protein nanoparticles for tumor active targeting. *Small* 8:2505-2514. 10.1002/smll.201200066

Liu X, Madhankumar AB, Slagle-Webb B, Sheehan JM, Surguladze N, and Connor JR. 2011. Heavy chain ferritin siRNA delivered by cationic liposomes increases sensitivity of cancer cells to chemotherapeutic agents. *Cancer Res* 71:2240-2249. 10.1158/0008-5472.Can-10-1375

Liu Z, Yang J, Liao Q, Lu Z, Jiang Q, Gong Y, Liu L, Peng H, Wang Q, and Zhang X. FTH1 indicates poor prognosis and promotes metastasis by regulating HMOX1 in head and neck squamous cell carcinoma, 25 October 2022, PREPRINT (Version 1) available at Research Square [https://doi.org/10.21203/rs.3.rs-2141682/v1].

Liu ZF, Yang J, Wei SP, Luo XG, Jiang QS, Chen T, and Gong YQ. 2020. Upregulated METTL3 in nasopharyngeal carcinoma enhances the motility of cancer cells. *Kaohsiung J Med Sci* 36:895-903. 10.1002/kjm2.12266

Lobello N, Biamonte F, Pisanu ME, Faniello MC, Jakopin Ž, Chiarella E, Giovannone ED,

Mancini R, Ciliberto G, Cuda G, and Costanzo F. 2016. Ferritin heavy chain is a negative regulator of ovarian cancer stem cell expansion and epithelial to mesenchymal transition. *Oncotarget* 7:62019-62033. 10.18632/oncotarget.11495

Lukina EA, Levina AA, Mokeeva RA, and Tokarev Yu N. 1993. The diagnostic significance of serum ferritin indices in patients with malignant and reactive histiocytosis. *British journal of haematology* 83:326-329.

Network CGA. 2015. Comprehensive genomic characterization of head and neck squamous cell carcinomas. *Nature* 517:576-582. 10.1038/nature14129

Rosager AM, Sørensen MD, Dahlrot RH, Hansen S, Schonberg DL, Rich JN, Lathia JD, and Kristensen BW. 2017. Transferrin receptor-1 and ferritin heavy and light chains in astrocytic brain tumors: Expression and prognostic value. *PloS one* 12:e0182954. 10.1371/journal.pone.0182954

Shan Z, Wei Z, and Shaikh ZA. 2018. Suppression of ferroportin expression by cadmium stimulates proliferation, EMT, and migration in triple-negative breast cancer cells. *Toxicology and Applied Pharmacology* 356:36-43. 10.1016/j.taap.2018.07.017

Su Q, Lei T, and Zhang M. 2017. Association of ferritin with prostate cancer. *Journal of BUON : official journal of the Balkan Union of Oncology* 22:766-770.

Tang D, Chen X, Kang R, and Kroemer G. 2021. Ferroptosis: molecular mechanisms and health implications. *Cell Res* 31:107-125. 10.1038/s41422-020-00441-1

Timoshnikov VA, Kobzeva TV, Polyakov NE, and Kontoghiorghes GJ. 2015. Inhibition of Fe(2+)- and Fe(3+)- induced hydroxyl radical production by the iron-chelating drug deferiprone. *Free radical biology & medicine* 78:118-122. 10.1016/j.freeradbiomed.2014.10.513

Torti SV, and Torti FM. 2013. Iron and cancer: more ore to be mined. *Nature reviews Cancer* 13:342-355. 10.1038/nrc3495

Wang W, Knovich MA, Coffman LG, Torti FM, and Torti SV. 2010. Serum ferritin: Past, present and future. *Biochimica et biophysica acta* 1800:760-769. 10.1016/j.bbagen.2010.03.011

Yang J, Gong Y, Jiang Q, Liu L, Li S, Zhou Q, Huang F, and Liu Z. 2020. Circular RNA Expression Profiles in Nasopharyngeal Carcinoma by Sequence Analysis. *Front Oncol* 10:601. 10.3389/fonc.2020.00601

Zhou J, Zhou Q, Shu G, Wang X, Lu Y, Chen H, Hu T, Cai J, Du Y, and Yu R. 2020. Dual-Effect of Magnetic Resonance Imaging Reporter Gene in Diagnosis and Treatment of Hepatocellular Carcinoma. *Int J Nanomedicine* 15:7235-7249. 10.2147/ijn.S257628

Figure 1

The workflow framework of this study.

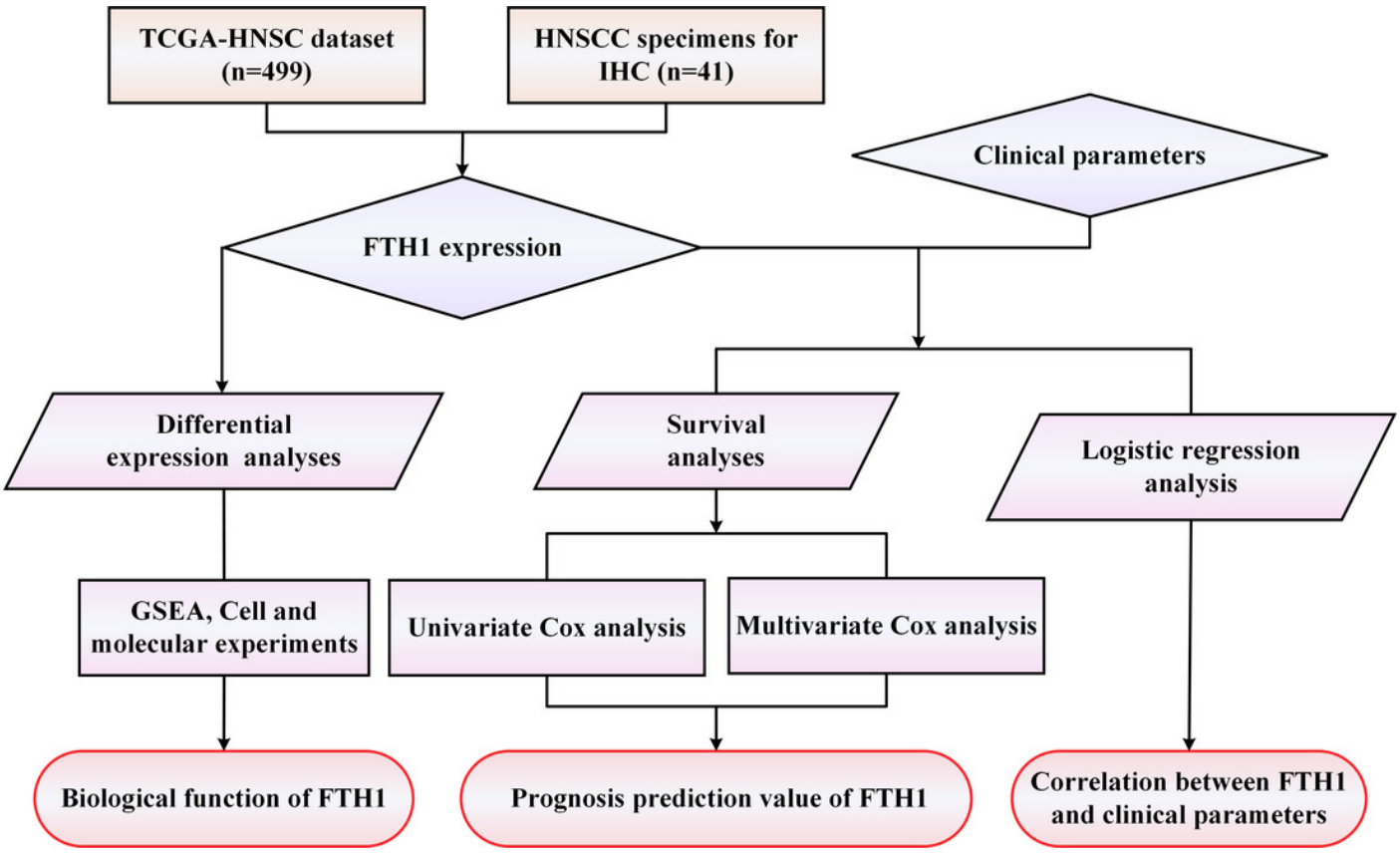

Figure 2

Elevated expression of FTH1 in HNSCC tissues.

(A) Differential expression of FTH1 in HNSCC and adjacent normal tissues in TCGA dataset. (B) Paired difference analysis of FTH1 mRNA expression in TCGA-HNSCC dataset. (C) The protein level of FTH1 in HNSCC cell lines and immortalized non-malignant cell line DOK was tested by western blot. Representative IHC staining demonstrates the expression of the FTH1 protein in adjacent normal (D) and HNSCC (E) tissues (100μm: 200×, 50μm: 400×). (F) The IHC score was significantly higher in HNSCC tissues than in adjacent tissues. *** $P < 0.001$.

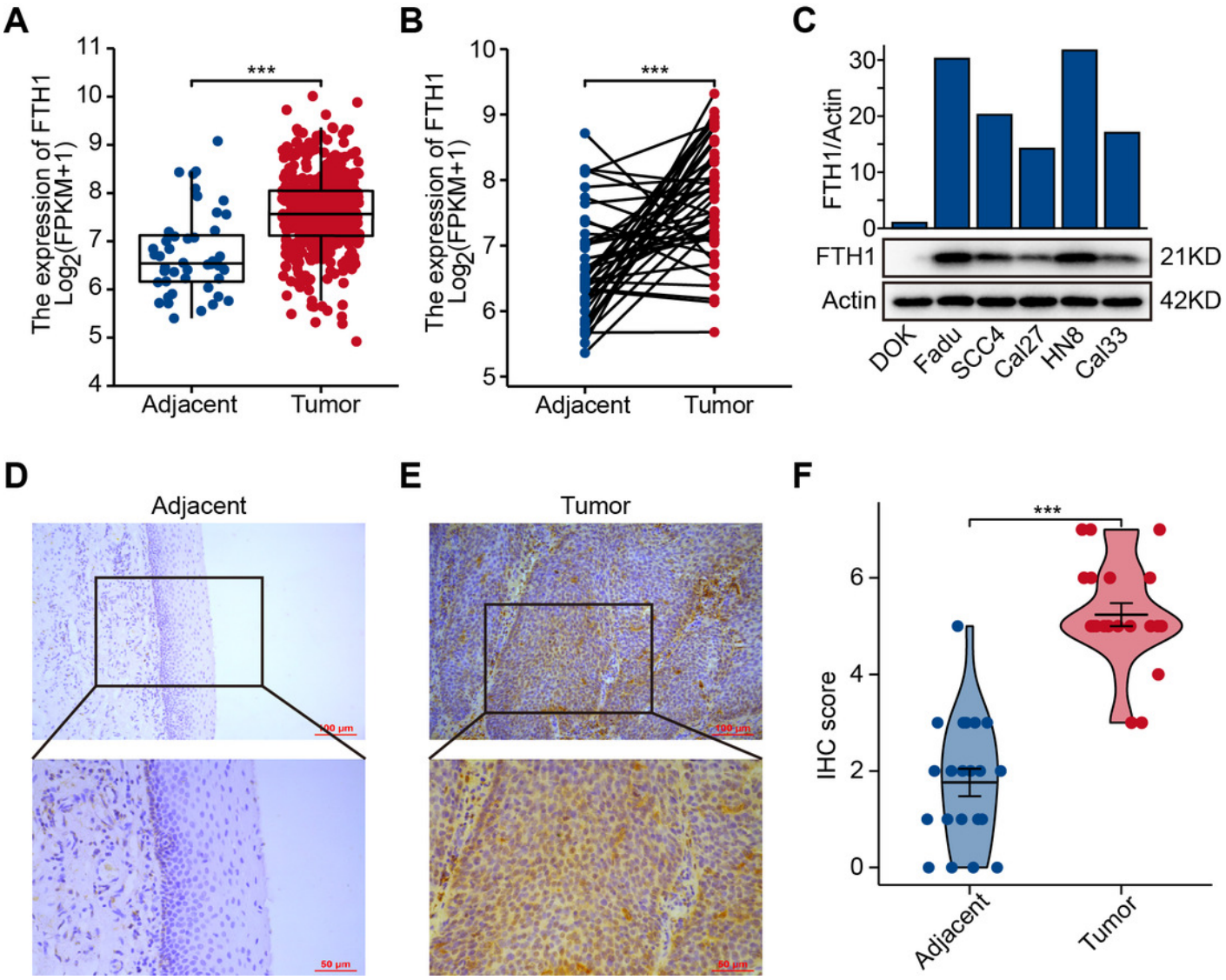
A
B
C
D
E
F
The expression of FTH1 Log2(FPKM+1)
***
Adjacent
Tumor
FTH1/Actin
FTH1
Actin
21KD
42KD
DOK
Fadu
SCC4
Cal27
HN8
Cal33
Adjacent
Tumor
IHC score

Figure 3

High levels of FTH1 predicts a worse prognosis of HNSCC patients.

Kaplan-Meier curves showed OS (A) and FDS (B) in HNSCC patients in terms of FTH1 expression.

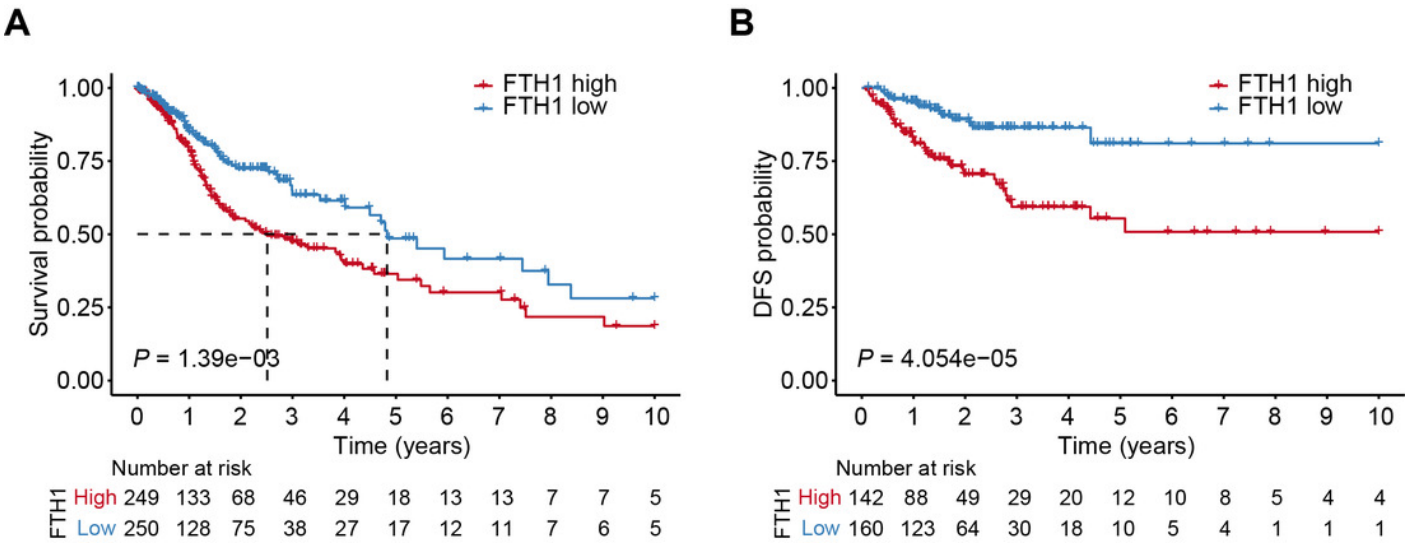

Figure 4

Correlation between FTH1 expression and clinicopathologic parameters.

Distribution of the FTH1 expression stratified by clinicopathologic parameters: (A) pathological grade (G1&2 and G3&4), (B) T stage (T1&2 and T3&4), (C) N stage (N0 and N+), (D) M stage (M0 and M1), (E) clinical stage (Stage I&II and Stage III&IV), (F) Age (<=60 and >60), (G) Gender (Female and Male), (H) smoking (No and Yes), (I) Alcohohistory (No and Yes). ns $P > 0.05$; * $P < 0.05$; ** $P < 0.01$; *** $P < 0.001$.

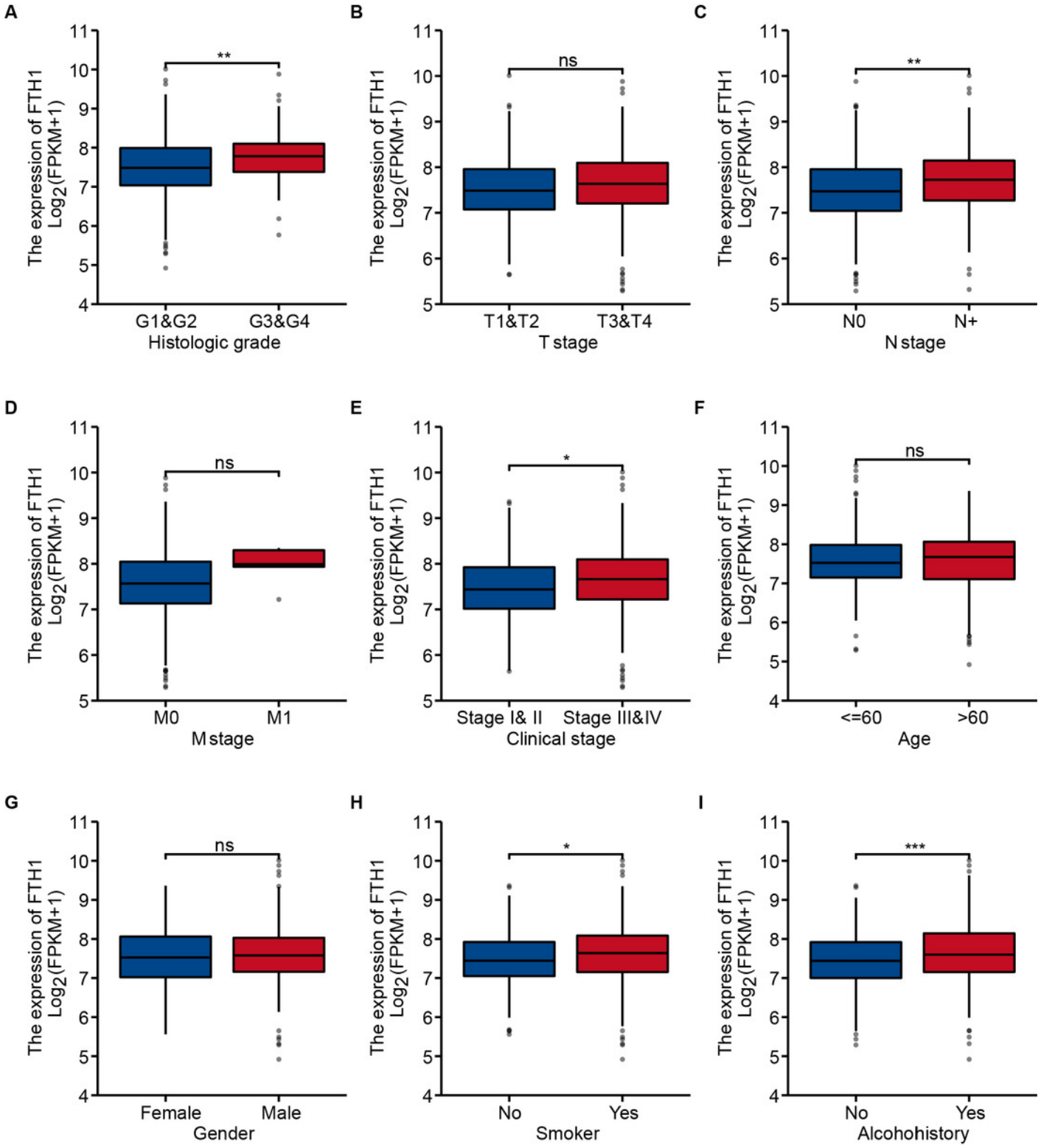
A
B
C
D
E
F
G
H
I
The expression of FTH1 Log2(FPKM+1)
**
ns
**
ns
*
ns
ns
*
***
G1&G2
G3&G4
Histologic grade
T1&T2
T3&T4
T stage
N0
N+
N stage
M0
M1
M stage
Stage I& II
Stage III&IV
Clinical stage
<=60
>60
Age
Female
Male
Gender
No
Yes
Smoker
No
Yes
Alcohohistory

Figure 5

Stratified Kaplan-Meier analysis for OS in HNSCC patients.

Stratified Kaplan-Meier analysis for OS with the differential clinical features, (A) Grade 1+2, (B) Grade 3+4, (C) N0, (D) N+, (E) Stage I+II, (F) Stage III+IV, (G) smoking, (H) no smoking, related to FTH1 expression in HNSCC patients.

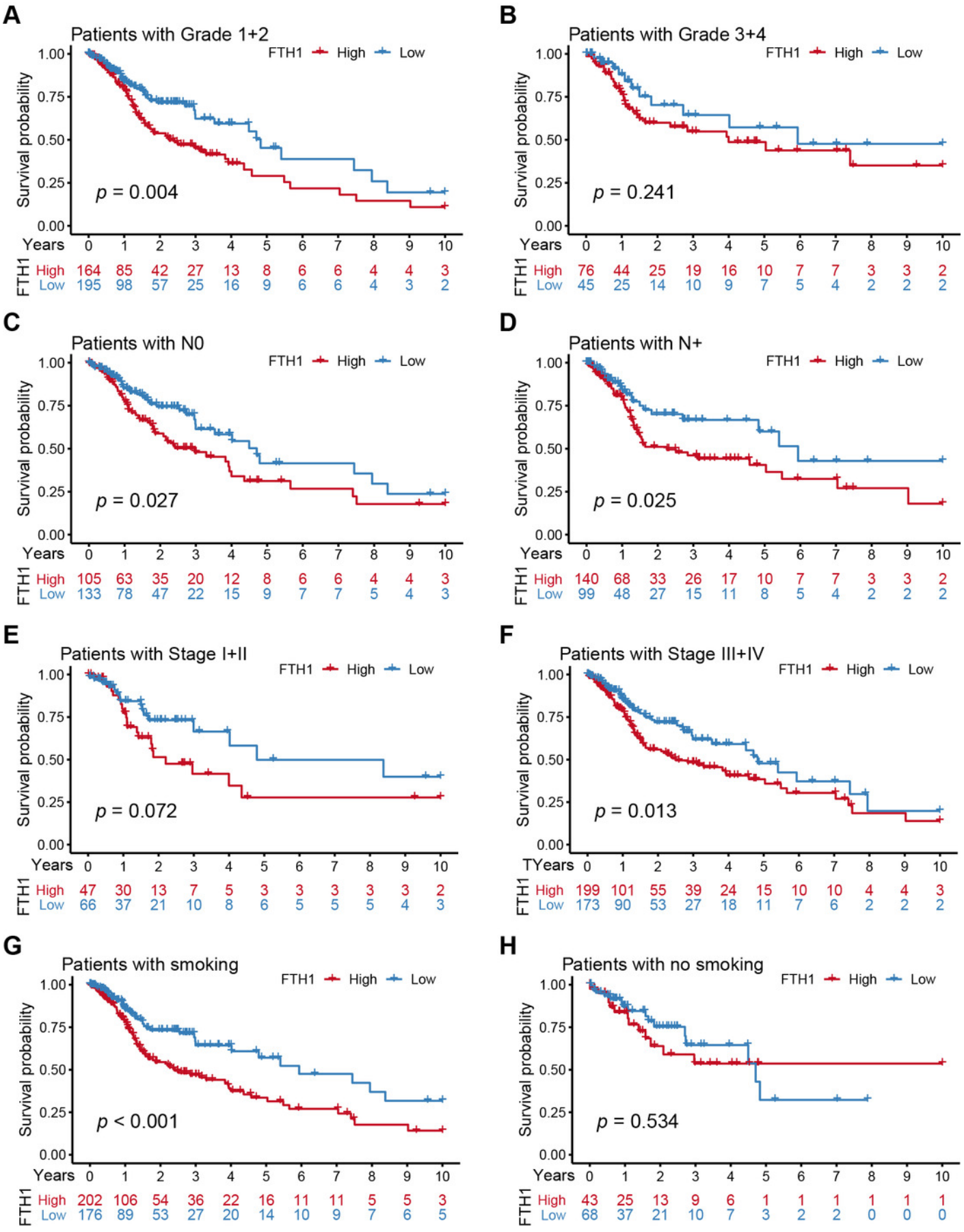
A
Patients with Grade 1+2
FTH1 High Low
Survival probability
p = 0.004
Years 0 1 2 3 4 5 6 7 8 9 10
FTH1 High 164 85 42 27 13 8 6 6 4 4 3
FTH1 Low 195 98 57 25 16 9 6 6 4 3 2
B
Patients with Grade 3+4
FTH1 High Low
Survival probability
p = 0.241
Years 0 1 2 3 4 5 6 7 8 9 10
FTH1 High 76 44 25 19 16 10 7 7 3 3 2
FTH1 Low 45 25 14 10 9 7 5 4 2 2 2
C
Patients with N0
FTH1 High Low
Survival probability
p = 0.027
Years 0 1 2 3 4 5 6 7 8 9 10
FTH1 High 105 63 35 20 12 8 6 6 4 4 3
FTH1 Low 133 78 47 22 15 9 7 7 5 4 3
D
Patients with N+
FTH1 High Low
Survival probability
p = 0.025
Years 0 1 2 3 4 5 6 7 8 9 10
FTH1 High 140 68 33 26 17 10 7 7 3 3 2
FTH1 Low 99 48 27 15 11 8 5 4 2 2 2
E
Patients with Stage I+II
FTH1 High Low
Survival probability
p = 0.072
Years 0 1 2 3 4 5 6 7 8 9 10
FTH1 High 47 30 13 7 5 3 3 3 3 3 2
FTH1 Low 66 37 21 10 8 6 5 5 5 4 3
F
Patients with Stage III+IV
FTH1 High Low
Survival probability
p = 0.013
TYears 0 1 2 3 4 5 6 7 8 9 10
FTH1 High 199 101 55 39 24 15 10 10 4 4 3
FTH1 Low 173 90 53 27 18 11 7 6 2 2 2
G
Patients with smoking
FTH1 High Low
Survival probability
p < 0.001
Years 0 1 2 3 4 5 6 7 8 9 10
FTH1 High 202 106 54 36 22 16 11 11 5 5 3
FTH1 Low 176 89 53 27 20 14 10 9 7 6 5
H
Patients with no smoking
FTH1 High Low
Survival probability
p = 0.534
Years 0 1 2 3 4 5 6 7 8 9 10
FTH1 High 43 25 13 9 6 1 1 1 1 1 1
FTH1 Low 68 37 21 10 7 3 2 2 0 0 0

Figure 6

Stratified Kaplan-Meier analysis for DFS in HNSCC patients.

Stratified Kaplan-Meier analysis for DFS with the differential clinical features, (A) Grade 1+2, (B) Grade 3+4, (C) N0, (D) N+, (E) Stage I+II, (F) Stage III+IV, (G) smoking, (H) no smoking, related to FTH1 expression in HNSCC patients.

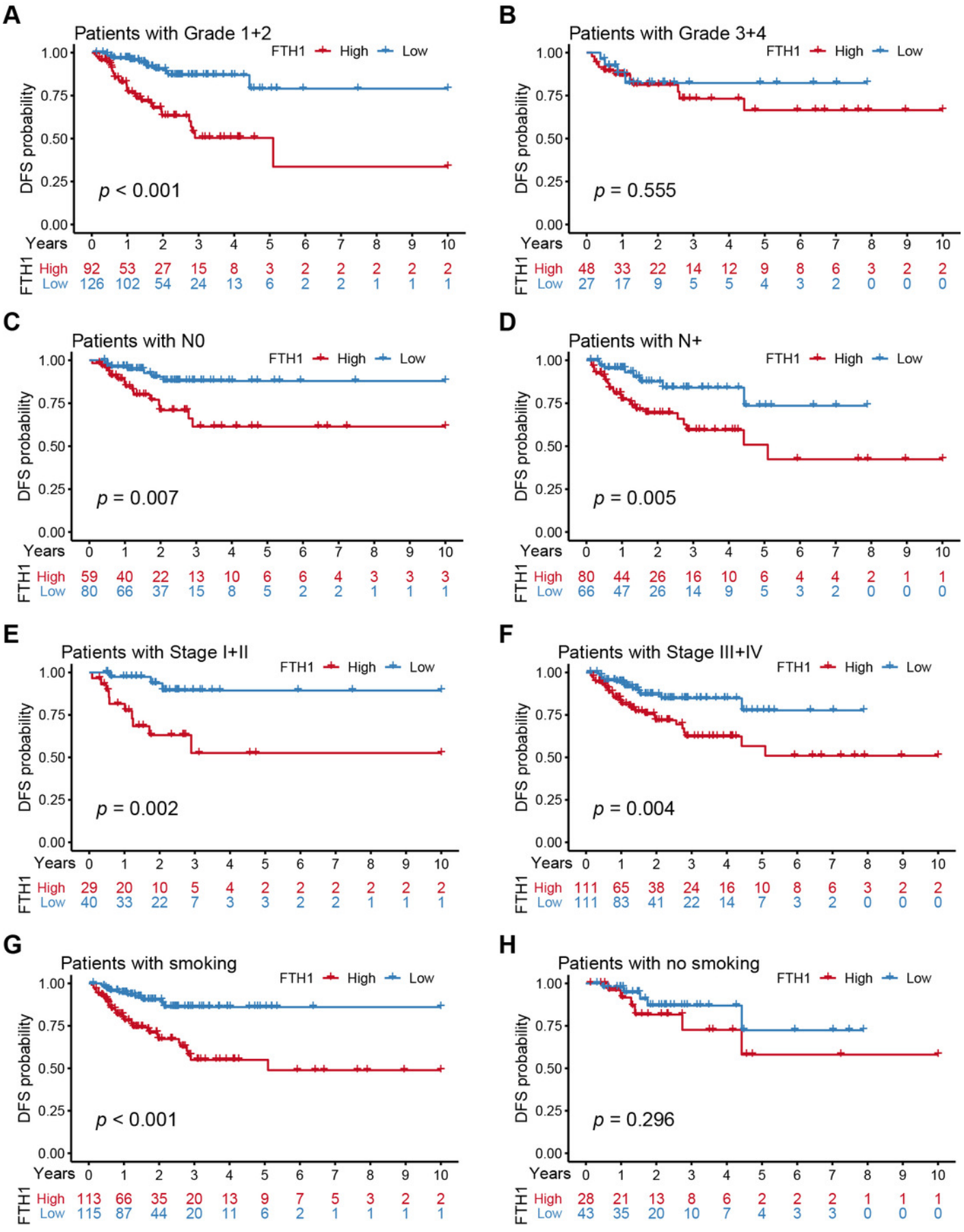
A
Patients with Grade 1+2
FTH1 High Low
DFS probability
p < 0.001
Years 0 1 2 3 4 5 6 7 8 9 10
FTH1 High 92 53 27 15 8 3 2 2 2 2 2
Low 126 102 54 24 13 6 2 2 1 1 1
B
Patients with Grade 3+4
FTH1 High Low
DFS probability
p = 0.555
Years 0 1 2 3 4 5 6 7 8 9 10
FTH1 High 48 33 22 14 12 9 8 6 3 2 2
Low 27 17 9 5 5 4 3 2 0 0 0
C
Patients with N0
FTH1 High Low
DFS probability
p = 0.007
Years 0 1 2 3 4 5 6 7 8 9 10
FTH1 High 59 40 22 13 10 6 6 4 3 3 3
Low 80 66 37 15 8 5 2 2 1 1 1
D
Patients with N+
FTH1 High Low
DFS probability
p = 0.005
Years 0 1 2 3 4 5 6 7 8 9 10
FTH1 High 80 44 26 16 10 6 4 4 2 1 1
Low 66 47 26 14 9 5 3 2 0 0 0
E
Patients with Stage I+II
FTH1 High Low
DFS probability
p = 0.002
Years 0 1 2 3 4 5 6 7 8 9 10
FTH1 High 29 20 10 5 4 2 2 2 2 2 2
Low 40 33 22 7 3 3 2 2 1 1 1
F
Patients with Stage III+IV
FTH1 High Low
DFS probability
p = 0.004
Years 0 1 2 3 4 5 6 7 8 9 10
FTH1 High 111 65 38 24 16 10 8 6 3 2 2
Low 111 83 41 22 14 7 3 2 0 0 0
G
Patients with smoking
FTH1 High Low
DFS probability
p < 0.001
Years 0 1 2 3 4 5 6 7 8 9 10
FTH1 High 113 66 35 20 13 9 7 5 3 2 2
Low 115 87 44 20 11 6 2 1 1 1 1
H
Patients with no smoking
FTH1 High Low
DFS probability
p = 0.296
Years 0 1 2 3 4 5 6 7 8 9 10
FTH1 High 28 21 13 8 6 2 2 2 1 1 1
Low 43 35 20 10 7 4 3 3 0 0 0

Figure 7

Enrichment results from multiple GSEA.

(A) energy metabolism, (B) glycometabolism, (C) protein and amino metabolism, (D) other metabolisms, (E) cell adhesion and (F) motility and tumor-associated signal pathways.

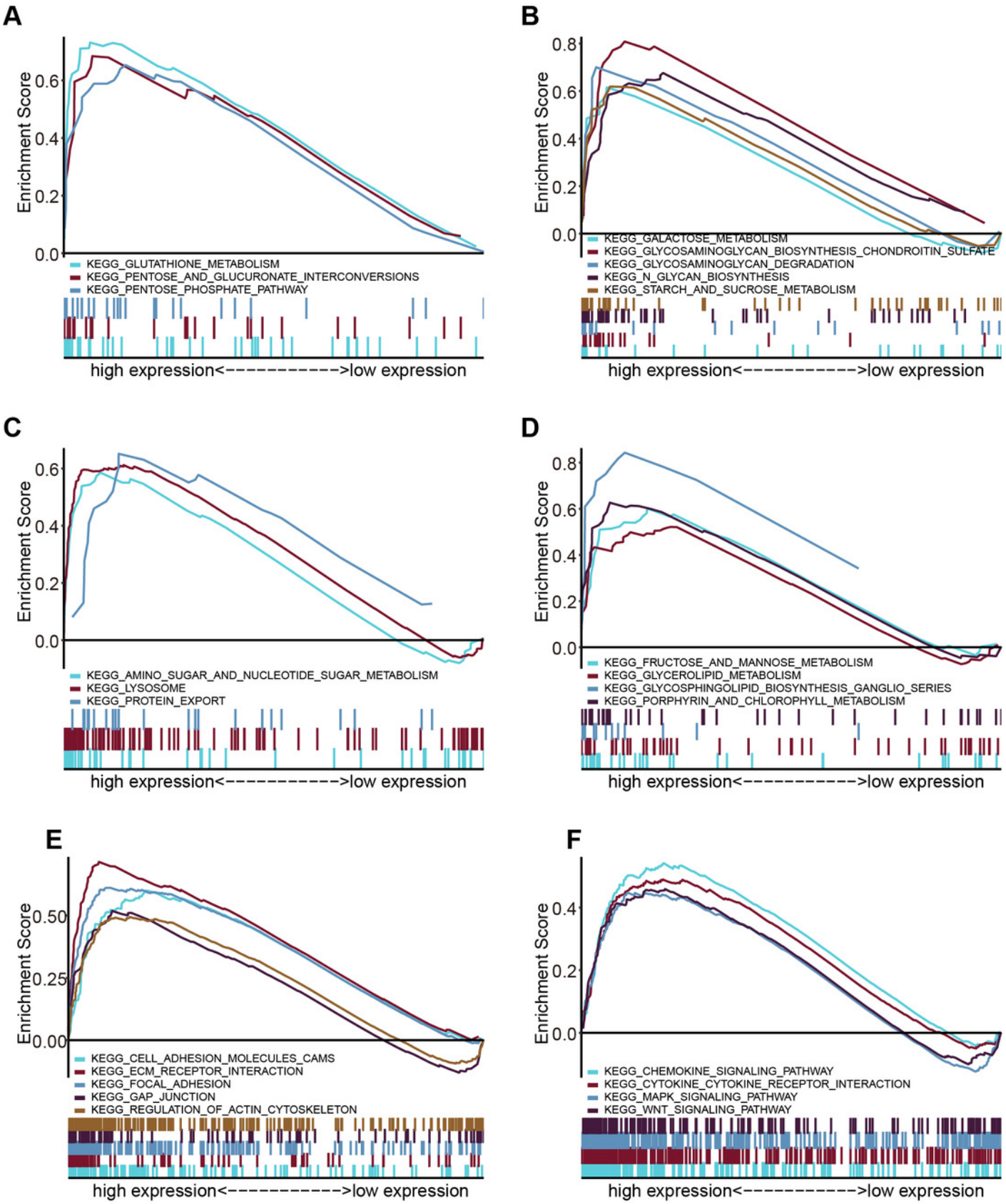
A
Enrichment Score
0.0
0.2
0.4
0.6
KEGG_GLUTATHIONE_METABOLISM
KEGG_PENTOSE_AND_GLUCURONATE_INTERCONVERSIONS
KEGG_PENTOSE_PHOSPHATE_PATHWAY
high expression<---------->low expression
B
Enrichment Score
0.0
0.2
0.4
0.6
0.8
KEGG_GALACTOSE_METABOLISM
KEGG_GLYCOSAMINOGLYCAN_BIOSYNTHESIS_CHONDROITIN_SULFATE
KEGG_GLYCOSAMINOGLYCAN_DEGRADATION
KEGG_N_GLYCAN_BIOSYNTHESIS
KEGG_STARCH_AND_SUCROSE_METABOLISM
high expression<---------->low expression
C
Enrichment Score
0.0
0.2
0.4
0.6
KEGG_AMINO_SUGAR_AND_NUCLEOTIDE_SUGAR_METABOLISM
KEGG_LYSOSOME
KEGG_PROTEIN_EXPORT
high expression<---------->low expression
D
Enrichment Score
0.0
0.2
0.4
0.6
0.8
KEGG_FRUCTOSE_AND_MANNOSE_METABOLISM
KEGG_GLYCEROLIPID_METABOLISM
KEGG_GLYCOSPHINGOLIPID_BIOSYNTHESIS_GANGLIO_SERIES
KEGG_PORPHYRIN_AND_CHLOROPHYLL_METABOLISM
high expression<---------->low expression
E
Enrichment Score
0.00
0.25
0.50
KEGG_CELL_ADHESION_MOLECULES_CAMS
KEGG_ECM_RECEPTOR_INTERACTION
KEGG_FOCAL_ADHESION
KEGG_GAP_JUNCTION
KEGG_REGULATION_OF_ACTIN_CYTOSKELETON
high expression<---------->low expression
F
Enrichment Score
0.0
0.2
0.4
KEGG_CHEMOKINE_SIGNALING_PATHWAY
KEGG_CYTOKINE_CYTOKINE_RECEPTOR_INTERACTION
KEGG_MAPK_SIGNALING_PATHWAY
KEGG_WNT_SIGNALING_PATHWAY
high expression<---------->low expression

Figure 8

FTH1 inhibition suppressed HNSCC cell migration.

Migration ability of HNSCC cells (A-D) were tested and quantified by wound healing assay. Invasive ability was examined and quantified by Transwell invasion assay (E and F).

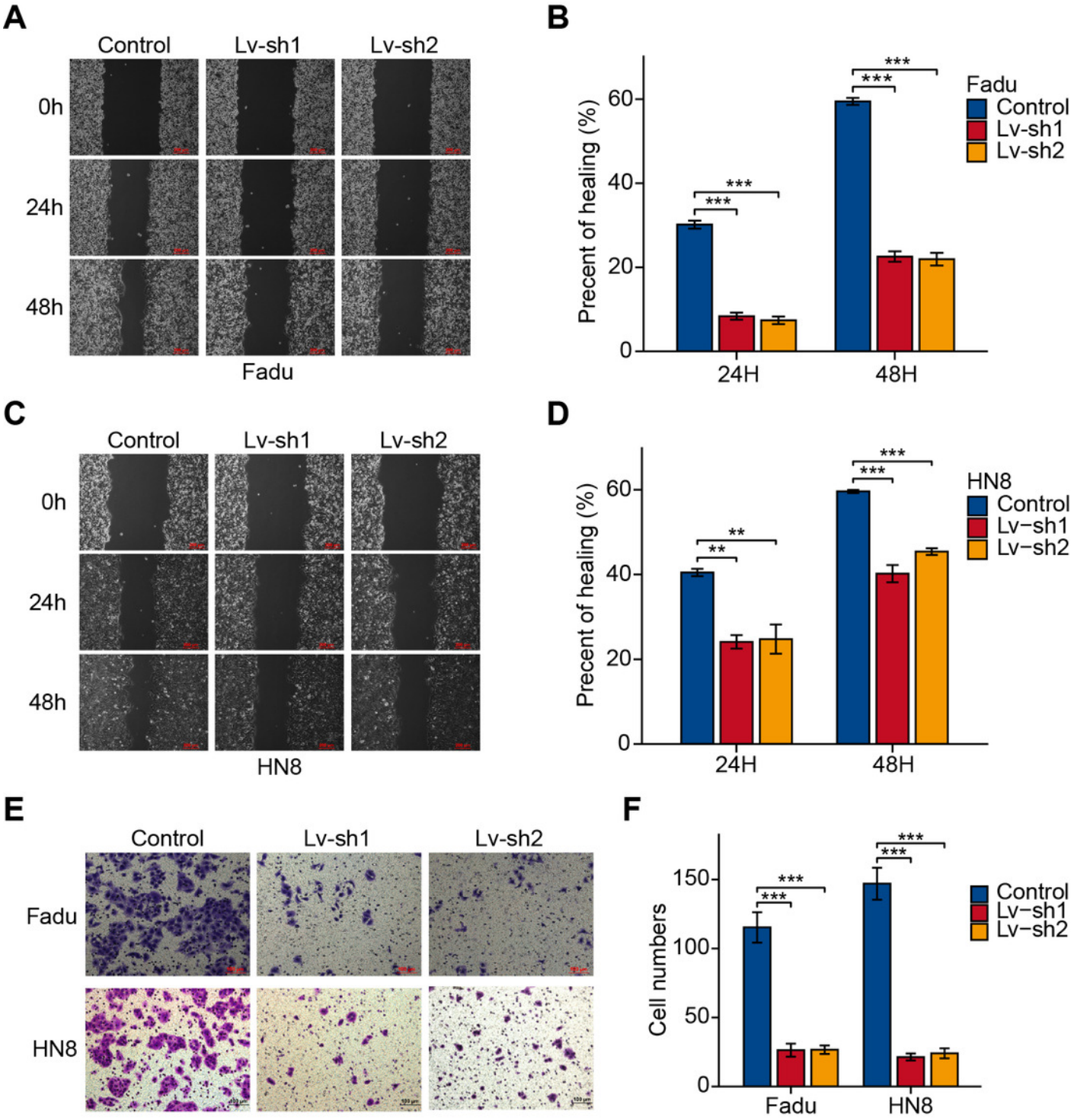
A
Control
Lv-sh1
Lv-sh2
0h
24h
48h
Fadu
B
Precent of healing (%)
60
40
20
0
***
***
***
***
24H
48H
Fadu
Control
Lv-sh1
Lv-sh2
C
Control
Lv-sh1
Lv-sh2
0h
24h
48h
HN8
D
Precent of healing (%)
60
40
20
0
**
**
***
***
24H
48H
HN8
Control
Lv-sh1
Lv-sh2
E
Control
Lv-sh1
Lv-sh2
Fadu
HN8
F
Cell numbers
150
100
50
0
***
***
***
***
Fadu
HN8
Control
Lv-sh1
Lv-sh2

Figure 9

FTH1 knockdown suppresses HNSCC EMT.

(A and B) Western blotting was performed to examine the expression of E-cadherin, N-cadherin and vimentin proteins after FTH1 depletion.

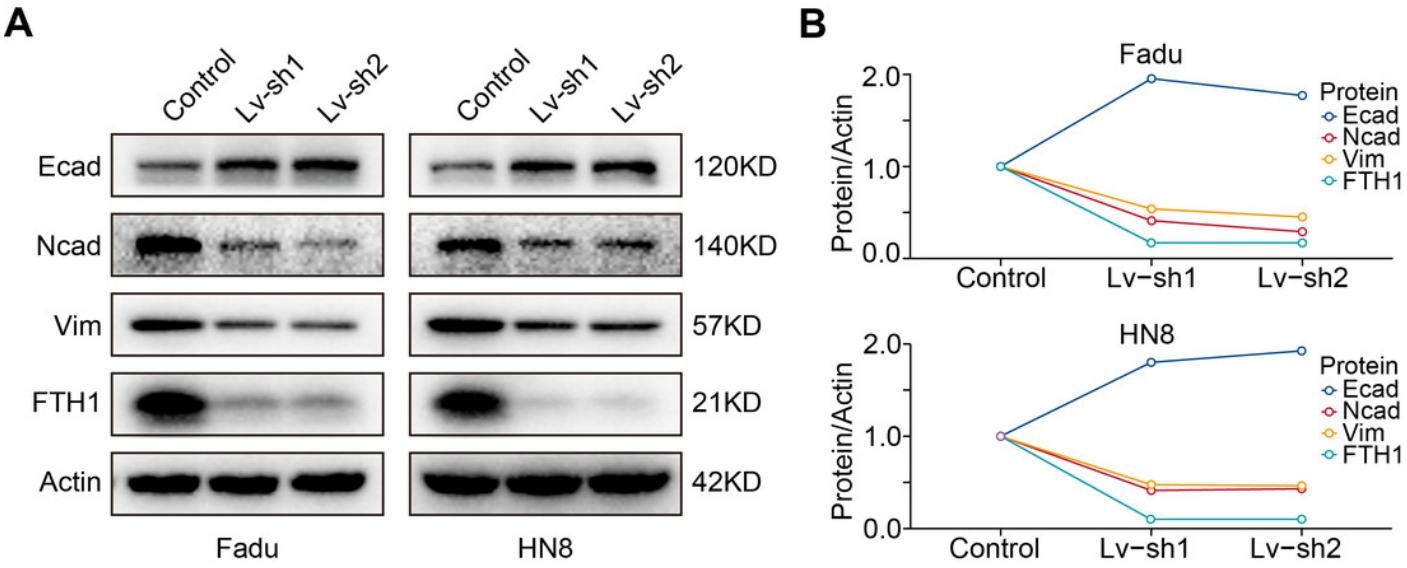

Table 1(on next page)

Clinicopathologic parameters of TCGA HNSCC patients.

Table 1 Clinicopathologic parameters of TCGA HNSCC patients.

Clinicopathologic parameters	FTH1 expression				*P*-value
	Low (n=250)		High (n=249)		
Age					0.177
<60	118	23.65%	102	20.44%	
>=60	132	26.45%	147	29.46%	
Gender					0.418
Female	71	14.23%	62	12.42%	
Male	179	35.87%	187	37.47%	
Smoker					**0.009**
No	68	13.63%	43	8.62%	
Yes	177	35.47%	201	40.28%	
Alcohol history					0.059
No	34	6.81%	21	4.21%	
Yes	69	13.83%	80	16.03%	
Histologic grade					**0.001**
G1 + G2	196	39.28%	163	32.67%	
G3 + G4	45	9.02%	76	15.23%	
T stage					0.186
T1 + T2	94	18.84%	81	16.23%	
T3 + T4	146	29.26%	163	32.67%	
N stage					**0.001**
N0	99	19.84%	140	28.06%	
N1-N3	134	26.85%	104	20.84%	
M stage					0.372
M0	234	46.89%	235	47.09%	
M1	1	0.20%	4	0.80%	
Clinical stage					**0.018**
Stage I + Stage II	67	13.43%	46	9.22%	
Stage III + Stage IV	173	34.67%	199	39.88%	
OS event					**<0.001**
Alive	186	37.27%	147	29.46%	
Dead	64	12.83%	102	20.44%	
DFS event					**<0.001**
Free	184	36.87%	132	26.45%	
No	52	10.42%	86	17.23%	

Table 2(on next page)

Correlation between the clinicopathologic parameters and FTH1 expression (logistic regression).

Table 2 Correlation between the clinicopathologic parameters and FTH1 expression (logistic regression).

Parameters	Total (n)	Odds Ratio (OR)	*P*-value
Age (>60 vs. <=60)	499	1.288 (0.904-1.838)	0.161
Gender (Male vs. Female)	499	1.196 (0.804-1.783)	0.377
Smoker (Yes vs. No)	489	1.796 (1.17-2.781)	**0.008**
Alcohol history (Yes vs. No)	489	1.877 (1.004-3.573)	0.051
Histologic grade (G3+4 vs. G1+2)	480	2.031 (1.335-3.117)	**0.001**
T stage (T3+4 vs. T1+2)	484	1.296 (0.894-1.881)	0.172
N stage (N+ vs. N0)	477	1.822 (1.269-2.625)	**0.001**
M stage (M1 vs. M0)	474	3.983 (0.584-78.228)	0.218
Clinical stage (Stage III+ IV vs. Stage I+ II)	485	1.675 (1.096-2.579)	**0.018**

Table 3(on next page)

Univariate and multivariate cox regression of OS and clinicopathologic parameters in HNSCC patients.

Table 3 Univariate and multivariate cox regression of OS and clinicopathologic parameters in HNSCC patients.

Parameters	Univariate analysis		Multivariate analysis	
	HR (95% CI)	*P*-value	HR (95% CI)	*P*-value
Age (>60 vs. <=60)	1.252 (0.956-1.639)	0.102		
Gender (Male vs. Female)	0.764 (0.574-1.018)	0.066		
Smoker (Yes vs. No)	1.089 (0.778-1.525)	0.618		
Alcohol history (Yes vs. No)	0.952 (0.716-1.265)	0.733		
Grade (G3+4 vs. G1+2)	0.939 (0.688-1.282)	0.692		
T stage (T3+4 vs. T1+2)	1.245 (0.932-1.661)	0.137		
N stage (N+ vs. N0)	1.263 (0.964-1.653)	0.090		
M stage (M1 vs. M0)	3.721 (1.177-11.764)	**0.026**	3.547 (1.122-11.214)	**0.031**
Clinical stage (III+IV vs. I+II)	1.217 (0.878-1.688)	0.238		
FTH1 (High vs. Low)	1.646 (1.254-2.161)	**<0.001**	1.658 (1.252-2.194)	**<0.001**